

The first observations of wide-band interferometers and the spectra of relic gravitons

Massimo Giovannini ¹

Department of Physics, Theory Division, CERN, 1211 Geneva 23, Switzerland

INFN, Section of Milan-Bicocca, 20126 Milan, Italy

Abstract

Stochastic backgrounds of relic gravitons of cosmological origin extend from frequencies of the order of the aHz up to the GHz range. Since the temperature and polarization anisotropies constrain the low frequency normalization of the spectra, in the concordance paradigm the strain amplitude corresponding to the frequency window of wide-band interferometers turns out to be, approximately, nine orders of magnitude smaller than the astounding signal recently reported and attributed to a binary black hole merger. The backgrounds of relic gravitons expected from the early Universe are compared with the stochastic foregrounds stemming from the estimated multiplicity of the astrophysical sources. It is suggested that while the astrophysical foregrounds are likely to dominate between few Hz and 10 kHz, relic gravitons with frequencies exceeding 100 kHz represent a potentially uncontaminated signal for the next generation of high-frequency detectors currently under scrutiny.

¹Electronic address: massimo.giovannini@cern.ch

Stochastic backgrounds of relic gravitons have been envisaged as a genuine general relativistic effect well before the formulation of any of the conventional models aiming at a specific account of the early stages of the evolution of our Universe [1]. Since the governing equations of the tensor modes of the geometry are not invariant under the Weyl rescaling of the four-dimensional metric, relic gravitational waves are amplified thanks to the pumping action of the space-time curvature itself. Prior to the pioneering investigations of Ref. [1] the wave equations of the tensor modes were believed to be Weyl-invariant as it happens in the case of chiral fermions and electromagnetic waves in four space-time dimensions. After nearly forty years of analyses and speculations, stochastic backgrounds of relic gravitons are now one of the most plausible predictions of general relativity and of various classes of inflationary models [2]. In the pivotal scenario the production of relic gravitons is characterized by decreasing frequency spectra whose amplitudes and slopes are simultaneously fixed (at the conventional pivot wavenumber $k_p = 0.002 \text{ Mpc}^{-1}$) by $r_T = \mathcal{A}_T/\mathcal{A}_\mathcal{R}$ where \mathcal{A}_T and $\mathcal{A}_\mathcal{R}$ denote, respectively, the amplitudes² of the tensor and of the scalar power spectra. The lowest frequency range of the graviton spectra is therefore $\mathcal{O}(\text{few})$ aHz ($1 \text{ aHz} = 10^{-18} \text{ Hz}$) and it corresponds to the pivot frequency $\nu_p = k_p/(2\pi) = 3.092 \text{ aHz}$. The maximal frequency range depends instead on the post-inflationary transition; in the sudden approximation, customarily adopted in the concordance lore, the highest frequency of the spectrum is a fraction of the GHz ($1 \text{ GHz} = 10^9 \text{ Hz}$):

$$\begin{aligned} \nu_{max} &= \frac{1}{4\pi} \left(2\pi r_T \mathcal{A}_\mathcal{R} \Omega_{\text{R}0} \right)^{1/4} \sqrt{H_0 M_P} \\ &= 0.3 \left(\frac{r_T}{0.1} \right)^{1/4} \left(\frac{\mathcal{A}_\mathcal{R}}{2.41 \times 10^{-9}} \right)^{1/4} \left(\frac{h_0^2 \Omega_{\text{R}0}}{4.15 \times 10^{-5}} \right)^{1/4} \text{ GHz}, \end{aligned} \quad (1)$$

where $\Omega_{\text{R}0}$ is the fraction of critical energy density attributed to massless particles (photons and neutrinos in the vanilla Λ CDM paradigm [3, 4]) while h_0 is the present value of the Hubble rate H_0 in units of $10^2 \text{ km}/(\text{sec} \times \text{Mpc})$. Equation (1) is derived by redshifting the frequency from the end of the inflationary epoch to the present time. At the end of inflation the maximal frequency of the spectrum coincides approximately with the Hubble rate during inflation. Today this frequency is clearly different and it depends, in principle, on the whole post-inflationary history. The simplest way to estimate this quantity is to consider the case where the reheating occurs suddenly: in this case the end of inflation coincides with the onset of the radiation dominated phase. Recalling that, in the sudden reheating approximation, the total redshift between the end of inflation and the present time is given by $2\sqrt{H_0 M_P} [2\Omega_{\text{R}0}/(\pi r_T \mathcal{A}_\mathcal{R})]^{1/4}$ the result of Eq. (1) follows immediately. This observation suggests that the early variations of the space-time curvature can therefore

²In the concordance paradigm (often dubbed Λ CDM paradigm where Λ denotes the dark energy component and CDM stands for the cold dark matter contribution) the spectral slope n_T and the slow-roll parameter ϵ are expressible in terms of r_T according to the so-called consistency relations stipulating that $n_T = -2\epsilon = -r_T/8$ [3, 4].

be assessed, with a fair degree of confidence, by scrutinizing the spectra of the relic gravitons at low but especially at high frequencies.

Whenever the (transverse and traceless) tensor modes of the four-dimensional geometry evolve in a homogeneous and isotropic background of Friedmann-Robertson-Walker type, each of the two tensor polarizations follows the action of a minimally coupled scalar field so that, ultimately, their energy density is³:

$$\mathcal{T}_0^0 = \frac{1}{8\ell_P^2 a^2} \left[\partial_\tau h_{ij} \partial_\tau h_{ij} + \partial_k h_{ij} \partial_k h_{ij} \right], \quad h_i^i = \partial_i h_j^i = 0, \quad \ell_P = \sqrt{8\pi G}, \quad (2)$$

where τ is the conformal time coordinate and ℓ_P is the Planck length. While different prescriptions can be used to assign the energy-momentum pseudo-tensor of the relic gravitons, they all coincide when the corresponding wavelengths are shorter than the Hubble radius (see last paper of [5] for a derivation of various pseudo-tensors and for their mutual comparison in different regimes). The result of Eq. (2) follows from the analysis of Ford and Parker (see second paper of Ref. [5]) but the Landau-Lifshitz approach leads to the same results in the regime of short wavelengths, as we shall briefly discuss later on.

The energy density of Eq. (2) also determines the tensor power spectrum $\mathcal{P}_T(k, \tau)$ measuring the amplitude of the two-point function at equal times in Fourier space⁴:

$$\langle h_{ij}(\vec{k}, \tau) h_{mn}(\vec{p}, \tau) \rangle = \frac{2\pi^2}{k^3} \mathcal{P}_T(k, \tau) \mathcal{S}_{ijmn}(\hat{k}) \delta^{(3)}(\vec{k} + \vec{p}), \quad (3)$$

where $\mathcal{S}_{ijmn}(\hat{k}) = [p_{mi}(\hat{k})p_{nj}(\hat{k}) + p_{mj}(\hat{k})p_{ni}(\hat{k}) - p_{ij}(\hat{k})p_{mn}(\hat{k})]/4$. The two-point function for the conformal time derivative of the amplitudes (i.e. $\langle \partial_\tau h_{ij} \partial_\tau h_{mn} \rangle$) is given by an expression formally analog to Eq. (3) but characterized by a different power spectrum denoted hereunder by \mathcal{Q}_T . With these specifications the energy density of the relic gravitons is simply $\rho_{gw} = \langle \mathcal{T}_0^0 \rangle$, where the average is taken over the quantum state minimizing the Hamiltonian of the relic gravitons. Along a complementary perspective the expectation value appearing in Eq. (3) can be viewed as an ensemble average over classical amplitudes with respect to a suitable stochastic process. In units of the critical energy density ρ_{crit} , the relation between the tensor power spectrum and the energy density per logarithmic⁵ interval of comoving wavenumber (i.e. the spectral energy density) is given by:

$$\begin{aligned} \Omega_{gw}(k, \tau) &= \frac{1}{\rho_{crit}} \frac{d\rho_{gw}}{d \ln k} = \frac{1}{24H^2 a^2} \left[k^2 \mathcal{P}_T(k, \tau) + \mathcal{Q}_T(k, \tau) \right] \\ &\rightarrow \frac{k^2}{12H^2 a^2} \mathcal{P}_T(k, \tau) \left[1 + \mathcal{O}\left(\frac{\mathcal{H}^2}{k^2}\right) \right], \quad k\tau \gg 1. \end{aligned} \quad (4)$$

³In the framework of the Λ CDM paradigm [3, 4], we shall assume a conformally flat background geometry $\bar{g}_{\mu\nu} = a^2(\tau)\eta_{\mu\nu}$ where $a(\tau)$ is the scale factor and $\eta_{\mu\nu}$ is the Minkowski metric with signature mostly minus; the tensor fluctuation of the geometry is defined as $\delta_t g_{ij} = -a^2 h_{ij}$.

⁴Note that $p_{ij}(\hat{k}) = (\delta_{ij} - \hat{k}_i \hat{k}_j)$ is the transverse projector.

⁵The natural logarithms will be denoted by “ln” while the common logarithms will be denoted by “log”.

The final result of Eq. (4) holds when the modes are inside the Hubble radius since, in this case, $\mathcal{Q}_T \rightarrow [k^2 \mathcal{P}_T(k, \tau) + \mathcal{O}(\mathcal{H}^2)]$. In the opposite limit (i.e. $k/\mathcal{H} \ll 1$) we have instead that $\mathcal{Q}_T(k, \tau) \rightarrow [\mathcal{H}^2 \mathcal{P}_T(k, \tau) + \mathcal{O}(k^2)]$ where, as usual, $\mathcal{H} = aH$. The energy densities (and pressures) derived within different approaches coincide, to leading order⁶, when the corresponding wavelengths are inside the Hubble radius, i.e. $k > \mathcal{H}$.

The tensor power spectrum, the spectral amplitude $S_h(\nu, \tau)$ (measured in units of Hz^{-1}) and the dimensionless strain amplitude are all related: since $\mathcal{P}_T(2\pi\nu, \tau) = 4\nu S_h(\nu, \tau)$, Eq. (4) also implies

$$S_h(\nu, \tau) = \frac{3\mathcal{H}^2}{4\pi^2\nu^3} \Omega_{gw}(\nu, \tau) \rightarrow 7.981 \times 10^{-43} \left(\frac{100 \text{ Hz}}{\nu} \right)^3 h_0^2 \Omega_{gw}(\nu, \tau_0) \text{ Hz}^{-1}, \quad (5)$$

where, as already remarked, $\nu = k/(2\pi)$ denotes the comoving frequency in natural units. Finally the dimensionless strain amplitude obeys $h_c^2(\nu, \tau_0) = \nu S_h(\nu, \tau_0)$ so that $h_c(\nu, \tau_0)$ becomes explicitly:

$$h_c(\nu, \tau_0) = 8.933 \times 10^{-21} \left(\frac{100 \text{ Hz}}{\nu} \right) \sqrt{h_0^2 \Omega_{gw}(\nu, \tau_0)}. \quad (6)$$

The conventional inflationary models followed by a sudden reheating imply, in the case $r_T = 0.1$ [3, 4], that $h_0^2 \Omega_{gw}(\nu, \tau_0) = \mathcal{O}(10^{-16.8})$ [6, 7]; we are considering here frequencies $\mathcal{O}(100 \text{ Hz})$ and we assume that the tensor spectral index does not run (see in this respect, the last paper of [10]). For the same frequency range⁷ (compatible with the sensitivity of wide-band interferometers) Eq. (6) gives $h_c = \mathcal{O}(10^{-29})$: while this estimate consistently assumes $r_T = \mathcal{O}(0.1)$, future determinations of r_T might even determine an absolute normalization of the spectra at the pivot frequency ν_p .

The recent detection of gravitational waves reported by the LIGO/Virgo Collaboration [8] corresponds to a dimensionless strain amplitude $h_c = \mathcal{O}(10^{-21})$ which is between eight and nine orders of magnitude larger than the stochastic background produced by the conventional inflationary models predicting, from Eq. (6), $h_c = \mathcal{O}(10^{-29})$. The observed burst of gravitational radiation (attributed to a merger of black holes) does not have an electromagnetic counterpart: both the Swift and the Fermi LAT (Large Area Telescope) satellites searched, without success, in the optical, ultraviolet, x -rays and γ -rays [9]. This strategy could be useful for the near future insofar as only with the direct observation of a specific

⁶In the case of the Ford-Parker energy-momentum pseudo-tensor [5] the numerical factor in front of the correction $\mathcal{O}(\mathcal{H}^2/k^2)$ in Eq. (4) is $1/2$. Using the Landau-Lifshitz approach the correction appearing in Eq. (4) is then given by $-7/2$ (instead of $1/2$).

⁷The operating window of wide-band interferometers is between few Hz and roughly 10 kHz. At low frequencies the seismic noise dominates while at intermediate and high frequencies the thermal and shot noises dominate. Barring for further suppressions of the signal to noise ratio due to the overlap reduction function (accounting for the relative location of the two correlated interferometers) the maximal sensitivity occurs for $\nu = \mathcal{O}(100) \text{ Hz}$ and this will be the fiducial frequency adopted throughout this discussion (see e.g. first three papers of Ref. [7] and references therein).

electromagnetic counterpart to the gravitational signal it will be plausible to infer that gravitational waves travel at the speed of light (at least within a cocoon corresponding to the distance of the source). Absent direct confirmations of the LIGO/Virgo results, there are reasonable hopes that many more bursts of similar kind will be eventually observed with the forthcoming observational campaigns. Depending on the estimates, the rates of black hole mergers range from $\mathcal{O}(50) \text{ Gpc}^{-3} \text{ yr}^{-1}$ to $\mathcal{O}(300) \text{ Gpc}^{-3} \text{ yr}^{-1}$. If this is the case we can not only expect to have many more signals but also a potentially new stochastic foreground coming from many unresolved sources of gravitational radiation. The typical amplitude of this hypothetical (and not yet detected) gravitational wave foreground will lead to⁸

$$h_0^2 \Omega_{gw}^{(for)} = 4.9 \times 10^{-10} \left(\frac{h_0}{0.67} \right)^2 \left(\frac{\nu}{25 \text{ Hz}} \right)^{2/3}, \quad 25 \text{ Hz} < \nu \leq 100 \text{ Hz}. \quad (7)$$

The stochastic foreground of Eq. (7) can potentially mask the stochastic background of relic gravitons coming from the early Universe. Indeed, we shall now show that the relic graviton backgrounds of primordial origin will always be smaller than the plausible expectations Eq. (7). However we shall also demonstrate that for frequencies exceeding 10 kHz the preceding conclusion can be evaded.

To scrutinize the high-frequency behavior of the spectra and before the explicit numerical results, it is useful to consider the following approximate parametrization for the relic component⁹:

$$h_0^2 \Omega_{gw}(\nu, \tau_0) = \mathcal{N}_\rho(r_T, \Omega_{R0}) T_{low}^2(\nu/\nu_{eq}, R_\nu) T_{high}^2(\nu/\nu_s, \alpha) \left(\frac{\nu}{\nu_p} \right)^{n_T} e^{-2\beta\nu/\nu_{max}}, \quad (8)$$

$$\mathcal{N}_\rho(r_T, \Omega_{R0}) = 4.165 \times 10^{-15} r_T \left(\frac{h_0^2 \Omega_{R0}}{4.15 \times 10^{-5}} \right), \quad (9)$$

where the parameter $\beta = \mathcal{O}(1)$ depends upon the width of the transition between the inflationary phase and the subsequent radiation dominated phase; for different widths of the post-inflationary transition we can estimate $0.5 \leq \beta \leq 6.3$ [7]. The maximal frequency ν_{max} appearing in Eq. (9) has been already introduced in Eq. (1) while ν_{eq} is defined as:

$$\nu_{eq} = 1.317 \times 10^{-17} \left(\frac{h_0^2 \Omega_{M0}}{0.1364} \right) \left(\frac{h_0^2 \Omega_{R0}}{4.15 \times 10^{-5}} \right)^{-1/2} \text{ Hz}, \quad (10)$$

where Ω_{M0} denotes the present critical fraction of dusty matter in the Λ CDM paradigm.

In Eq. (9) T_{low} and T_{high} denote, respectively, the transfer functions at low and high frequencies. To transfer the spectrum inside the Hubble radius the procedure is to integrate numerically the equations of the tensor modes. This procedure for the derivation of T_{low} and

⁸We assume the Planck determination of h_0 and the expectations published in [8] for Ω_{gw} , namely $\Omega_{gw} = 1.1_{-0.9}^{2.7} \times 10^{-9} [\nu/(25 \text{ Hz})]^{2/3}$ for $25 \text{ Hz} < \nu \leq 100 \text{ Hz}$. For $\nu > 100 \text{ Hz}$ the signal is exponentially suppressed (see, in particular, the last paper of Ref. [8]).

⁹Note that R_ν denotes the fraction of neutrinos in the radiation plasma i.e. $R_\nu = r_\nu/(r_\nu + 1)$ where $r_\nu = \rho_\nu/\rho_\gamma = 0.681(N_\nu/3)$ and N_ν is the number of massless neutrino families.

T_{high} has been discussed in detail in the last paper of Ref. [6]. Approximations to the full transfer function (valid in the case of spectra produced during a stiff phase and in a waterfall transition) have been derived, respectively in Ref. [10] (see in particular second and third papers) and in the fourth paper of Ref. [7]. In the simple limit $R_\nu \rightarrow 0$ the transfer function across equality is given by [6]:

$$T_{low}(\nu/\nu_{eq}, 0) = \sqrt{1 + c_1 \left(\frac{\nu_{eq}}{\nu}\right) + b_1 \left(\frac{\nu_{eq}}{\nu}\right)^2}, \quad c_1 = 0.5238, \quad b_1 = 0.3537. \quad (11)$$

Similarly, denoting with ν_s the frequency at which the approximate scale invariance of the spectral energy density is broken we will have that $T_{high}^2 \rightarrow 1$ for $\nu \ll \nu_s$ while $T_{high}^2 \rightarrow (\nu/\nu_s)^\alpha$ for $\nu \gg \nu_s$. Potential violations of approximate scale-invariance for frequencies larger than a putative frequency ν_s arise in various situations including a prolonged stiff post-inflationary phase, a delayed reheating or even the presence of spectator fields triggering waterfall transitions [10]. In what follows ν_s will be referred to as the frequency of the ankle since it defines the beginning of the high-frequency branch where the spectral energy density can be sharply increasing. According to Eq. (11), $T_{low} \rightarrow 1$ for $\nu \gg \nu_{eq}$ but the realistic situations further suppressions are expected. At least two effects are not captured by Eq. (9): the free-streaming of collisionless species and the dark-energy transition. The neutrino free-streaming produces an effective anisotropic stress leading ultimately to an integro-differential equation (see, for instance, [11]). Assuming that the only collisionless species in the thermal history of the Universe are the neutrinos (which are massless in the concordance paradigm [3, 4]), the amount of suppression of $h_0^2 \Omega_{gw}$ for $\nu_{eq} < \nu < \nu_{bbn}$ can be parametrized by the function $\mathcal{F}(R_\nu) = 1 - 0.539R_\nu + 0.134R_\nu^2$ where ν_{bbn} is the comoving frequency that corresponding to the Hubble rate at nucleosynthesis:

$$\nu_{bbn} = 2.252 \times 10^{-11} \left(\frac{g_\rho}{10.75}\right)^{1/4} \left(\frac{T_{bbn}}{\text{MeV}}\right) \left(\frac{h_0^2 \Omega_{R0}}{4.15 \times 10^{-5}}\right)^{1/4} \text{ Hz} \simeq 0.01 \text{ nHz}, \quad (12)$$

where g_ρ denotes the effective number of relativistic degrees of freedom entering the total energy density of the plasma and T_{bbn} is the temperature of big-bang nucleosynthesis. The shallow suppression of $h_0^2 \Omega_{gw}$ in the range $\nu_{eq} < \nu < \nu_{bbn}$ is then proportional to $\mathcal{F}^2(0.405) = 0.645$ (for $N_\nu = 3$ and $R_\nu = 0.405$). The second effect not included in Eq. (1) is the damping effect associated with the (present) dominance of the dark energy component¹⁰. This effect is comparable with the suppression due to the neutrino free streaming¹¹ (see e.g. the last paper of Ref. [7]).

Thanks to the preceding semi-analytical arguments we can therefore infer that any departure from approximate scale-invariance beyond $\nu_s = \mathcal{O}(\text{nHz})$ will lead to a signal exceeding

¹⁰The redshift of Λ -dominance is given by $1 + z_\Lambda = (\Omega_{de}/\Omega_{M0})^{1/3}$; in the Λ CDM paradigm $\Omega_{de} \equiv \Omega_\Lambda$ and the damping across z_Λ reduces $h_0^2 \Omega_{gw}$ by a factor $(\Omega_{M0}/\Omega_\Lambda)^2 = \mathcal{O}(0.2)$.

¹¹There is a third effect reducing the quasi-flat plateau implied by Eq. (11) in the limit $\nu \gg \nu_{eq}$: the variation of the effective number of relativistic species [11, 7]. In the case of the minimal standard model this would imply that the reduction will be $\mathcal{O}(0.38)$.

astrophysical foregrounds but only for sufficiently large frequencies, i.e. above $\mathcal{O}(100\text{kHz})$. A large stochastic background for frequencies $\mathcal{O}(100\text{Hz})$ may correspond to the situation

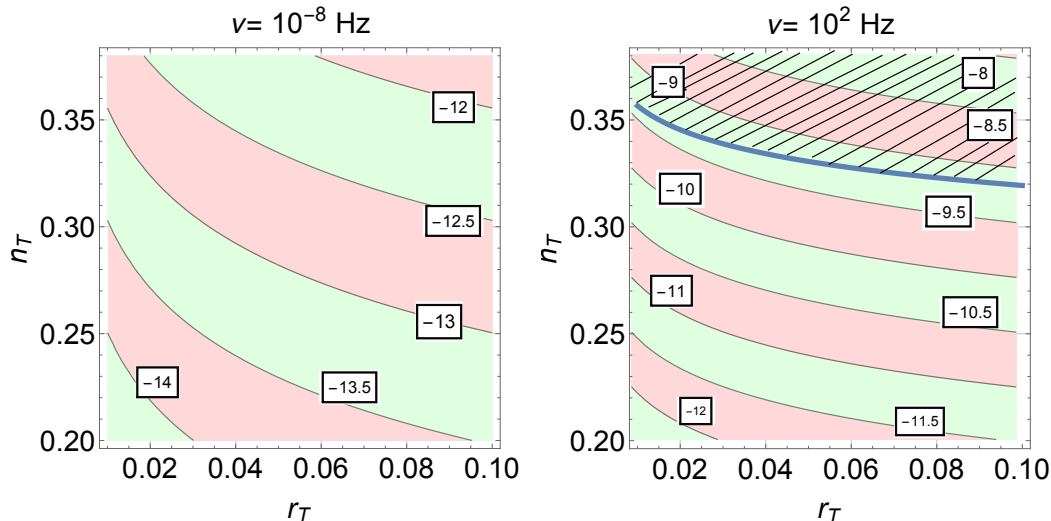


Figure 1: In both plots the contours correspond to a different value of the common logarithm of $h_0^2\Omega_{gw}$; r_T and n_T are independently assigned so that the consistency relation are violated. In the plot on the left ν corresponds to the pulsar timing frequency. In the plot on the right the big bang nucleosynthesis constraint at the LIGO/Virgo frequency is illustrated.

where $T_{high} \rightarrow 1$ but n_T and r_T are *independently assigned*. In this case the consistency relations are violated and we can see from Fig. 1 that the allowed region corresponds to $n_T < \mathcal{O}(0.37)$, assuming $r_T \leq 0.1$. In the plot on the left of Fig. 1 the pulsar timing measurements impose $\Omega_{gw}(\nu_{pulsar}, \tau_0) < 1.9 \times 10^{-8}$ which is an upper bound at a typical frequency $\nu_{pulsar} \simeq 10^{-8}\text{ Hz}$, roughly corresponding to the inverse of the observation time along which the pulsars timing has been monitored [12]. The Parkes pulsar timing array brings the limit down to 2.3×10^{-10} . While the plot on the left of Fig. 1 demonstrates that for $0.1 \leq n_T \leq 0.4$ the pulsar limits are safely satisfied, the plot on the right shows clearly that $h_0^2\Omega_{gw}$ can be sufficiently large for $\nu = 100\text{ Hz}$ but the resulting signal is of the same order of the presumed astrophysical foreground. Indeed, using $\nu = 100\text{ Hz}$, Eq. (7) implies that the stochastic foreground can be as large as $h_0^2\Omega_{gw}^{(for)} = 10^{-9.3}$: this value is barely compatible with the big bang nucleosynthesis bound illustrated in Fig. 1 with the shaded area. We remind that the big-bang nucleosynthesis limit sets an indirect constraint on the extra-relativistic species (and, among others, on the relic gravitons) at the time when light nuclei have been firstly formed [13]. For historical reasons this constraint is often expressed in terms of ΔN_ν representing the contribution of supplementary neutrino species but the extra-relativistic species do not need to be fermionic. If the additional species are relic gravitons we have:

$$h_0^2 \int_{\nu_{bbn}}^{\nu_{max}} \Omega_{gw}(\nu, \tau_0) d \ln \nu = 5.61 \times 10^{-6} \Delta N_\nu \left(\frac{h_0^2 \Omega_{\gamma 0}}{2.47 \times 10^{-5}} \right). \quad (13)$$

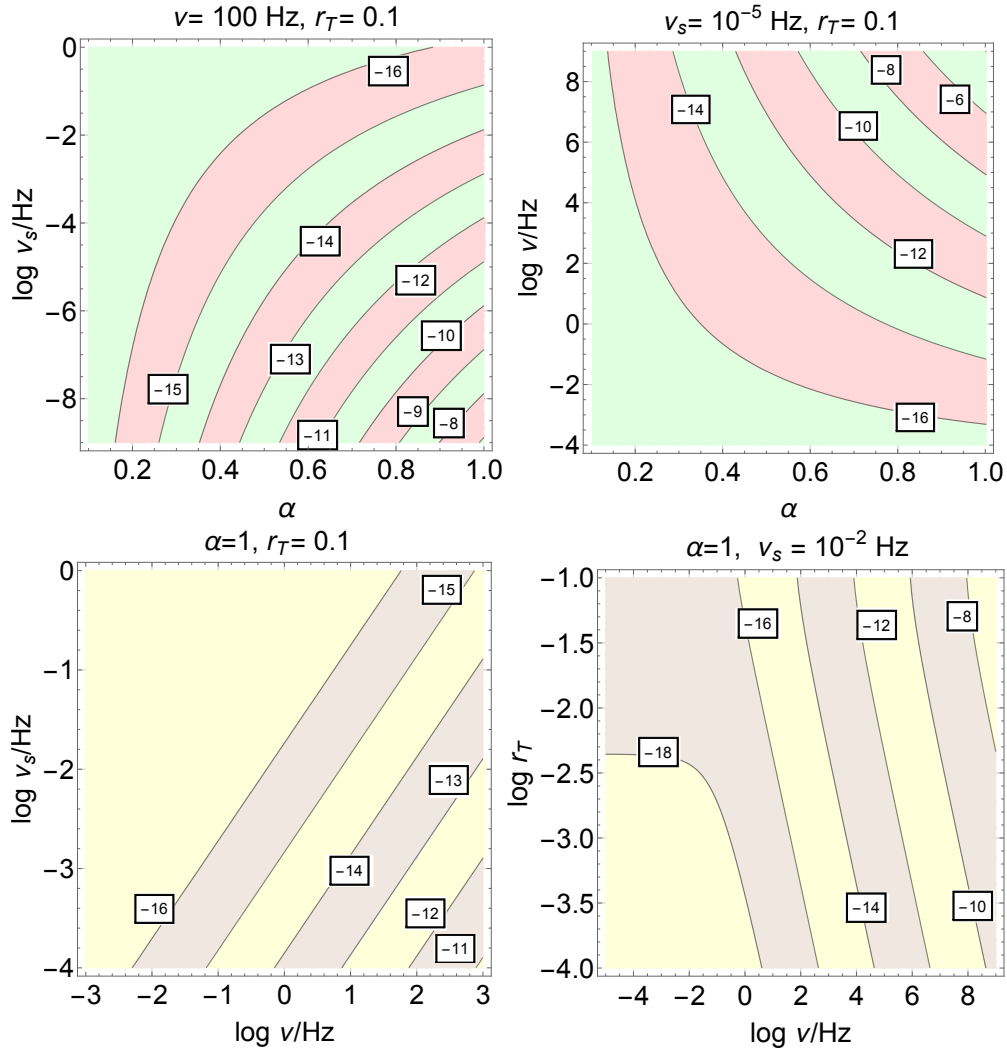


Figure 2: The same contours of Fig. 1 are illustrated in terms of $\log h_0^2 \Omega_{gw}$ for the four-dimensional parameter space consisting of the tensor to scalar ratio r_T , the spectral frequency ν , the frequency of the ankle ν_s and the high-frequency slope α . We have assumed the consistency relations and the other fiducial determinations [3, 4] of the remaining parameters of the Λ CDM scenario supplemented by tensors.

The bounds on ΔN_ν range from $\Delta N_\nu \leq 0.2$ to $\Delta N_\nu \leq 1$ implying that the integrated spectral density is between 10^{-6} and 10^{-5} . In the (r_T, n_T) plane of Fig. 1 the various labels on the curves denote the common logarithm of $h_0^2 \Omega_{gw}$ and the shaded area of the plot on the left is forbidden by the bound of Eq. (13). Since the relic graviton spectrum extends beyond 10 kHz with an increasing spectrum (i.e. $n_T > 0$) the integral of Eq. (13) is dominated by the highest frequency so that $h_0^2 \Omega_{gw}$ must be even smaller around 100 Hz.

The example of Fig. 1 is simple enough but unconventional: the positivity of the spectral index (i.e. $n_T > 0$) would demand a model based either on a non-minimal gravity theory

or on a violation of the dominant energy condition (see, in this respect, the third paper of [10]). The same features of Fig. 1 hold also when the consistency relations are not violated but the spectral energy density is not (approximately) scale-invariant in the high-frequency limit, as it happens in the case of Eq. (8). In Fig. 2 we illustrate the contours of constant $\log h_0^2 \Omega_{gw}$ for different choices of the four parameters involved in the discussion namely, ν , ν_s , r_T and α . The values of n_T and r_T are both constrained by the temperature and polarization anisotropies thanks to the consistency relations. The values of α and ν_s will instead be considered as free parameters with some plausible physical limitations. In case the inflationary phase is followed by an epoch where the plasma is dominated by a stiff source $\alpha \leq 1$ (up to logarithmic corrections); in the same context $\nu_s = \mathcal{O}(\text{mHz})$ (see first and second papers of [10]). Waterfall fields can also produce steep spectra with $\alpha > 1$ but with $\nu_s > \text{kHz}$ (see fourth paper of Ref. [7]). Since, at least in principle, the signal must be relevant for the LIGO/Virgo operating window, the latter case is less interesting than the former. This is why, in Fig. 2, we just reported the results for $\alpha \leq 1$. The spectral energy density in critical units always undershoots the value of the foreground of Eq. (7) for $\nu = \mathcal{O}(100)$ Hz (top left plot in Fig. 2). The regions where, apparently, the signal is large enough are excluded by the nucleosynthesis bound of Eq. (13). This happens in particular in the case of the plot on the top left corner of Fig. 2 where the curves leading to $h_0^2 \Omega_{gw} = \mathcal{O}(10^{-8})$ and $\mathcal{O}(10^{-6})$ are in fact excluded. The pulsar bound, in this context, does not play any role since $\nu_s \gg 10^{-8}$ Hz (see the bottom right plot of Fig. 2). The approximate choice of parameters $\alpha \rightarrow 1$ and $\nu_s = \mathcal{O}(10^{-2})\text{Hz}$ (top and bottom right plots in Fig. 2) always produces the largest signal.

There are some who might worry about the possibility that above the kHz many more sources could show up. This is difficult to foresee since the high-frequency detectors are not yet in an advanced stage of development (see following paragraph). From the theoretical viewpoint we would like to mention three interesting possibilities [14] and contrast them with the present findings. In the first paper of Ref. [14] the authors describe an interesting idea to detect gravity waves at high frequencies with particular attention to the frequency range of 50 – 300 kHz. As far as the possibility of a signal is concerned the authors only mention the effect of QCD axion in astrophysical stellar mass black holes. This signal occurs, according to the paper, for a typical frequency of 290 kHz (twice the mass of the axion) for a Peccei-Quinn scale 10^{16} GeV. The signal is coherent and monochromatic thus completely different from the stochastic backgrounds discussed in this paper. In the second reference of [14] the authors discuss potential signals of gravitational radiation (for frequencies larger than 100 Hz) arising in a model where two branes are connected by a black string. Finally in the third and fourth papers of Ref. [14] the authors suggest that, maybe, magnetized plasmas could produce intense gravitational waves. The frequencies appearing in this last paper of Ref. [14] range between 100 Hz and 100 kHz with rather uncertain amplitudes.

While the recent detection of gravitational radiation cannot be independently confirmed, the multiplicity of the observed events is bound to increase dramatically in the near future.

If this is the case, the presence of an astrophysical foreground of stochastically distributed amplitudes of gravitational waves seems to be unavoidable. These foregrounds are likely to mask the stochastic backgrounds of relic gravitons bearing the mark of the early variation of the Hubble expansion rate. For frequencies larger than the mHz the primeval spectra can be decreasing, quasi-flat or even increasing (with spiky shapes) mostly depending on post-inflationary evolution. While the astrophysical foregrounds will always be dominant at least between 25 and 100 Hz, over higher frequencies this conclusion can be evaded. The present analysis suggests that future plannings of space-borne interferometers (in the mHz range) of terrestrial networks (between few Hz and 10 kHz) should be usefully complemented by high-frequency instruments (such as microwave resonator or wave guide detectors [15]) operating above 10 kHz. The forthcoming generations of high-frequency detectors might be the sole hope of achieving a direct detection of cosmic backgrounds of relic gravitons free from foreseeable foreground contaminations.

References

- [1] L. P. Grishchuk, Sov. Phys. JETP **40**, 409 (1975) [Zh. Eksp. Teor. Fiz. **67**, 825 (1974)]; Annals N. Y. Acad. Sci. **302**, 439 (1977); A. A. Starobinsky, JETP Lett. **30**, 682 (1979).
- [2] V. A. Rubakov, M. V. Sazhin and A. V. Veryaskin, Phys. Lett. B **115**, 189 (1982); B. Allen, Phys. rev. D **37**, 2078 (1988); V. Sahni, Phys. Rev. D **42**, 453 (1990); L. P. Grishchuk and M. Solokhin, Phys. Rev. D **43**, 2566 (1991); M. Gasperini and M. Giovannini, Phys. Lett. B **282**, 36 (1992).
- [3] B. Gold *et al.*, *ibid.* **192**, 15 (2011); D. Larson, *et al.*, *ibid.* **192**, 16 (2011); C. L. Bennett *et al.*, *ibid.* **192**, 17 (2011); G. Hinshaw *et al.*, *ibid.* **208** 19 (2013); C. L. Bennett *et al.*, *ibid.* **208** 20 (2013).
- [4] P. A. R. Ade *et al.* [BICEP2 Collaboration], Phys. Rev. Lett. **112**, 241101 (2014); P. A. R. Ade *et al.* [Planck Collaboration], Astron. Astrophys. **571**, A22 (2014); Astron. Astrophys. **571**, A16 (2014); P. A. R. Ade *et al.* [Planck Collaboration], arXiv:1502.02114 [astro-ph.CO].
- [5] R. Isaacson, Phys. Rev. **166**, 1263 (1968); Phys. Rev. **166**, 1272 (1968); L. H. Ford and L. Parker, Phys. Rev. D **16**, 1601 (1977); Phys. Rev. D **16**, 245 (1977); L. Abramo, Phys. Rev. D **60**, 064004 (1999); M. Giovannini, Phys. Rev. D **73**, 083505 (2006).
- [6] M. S. Turner, M. J. White and J. E. Lidsey, Phys. Rev. D **48**, 4613 (1993); Y. Zhang, W. Zhao, T. Xia and Y. Yuan, Phys. Rev. D **74**, 083006 (2006); S. Chongchitnan and G. Efstathiou, Phys. Rev. D **73**, 083511 (2006); M. Giovannini, Phys. Lett. B **668**, 44 (2008); Class. Quant. Grav. **26**, 045004 (2009).

- [7] D. Babusci and M. Giovannini, Phys. Rev. D **60**, 083511 (1999); Class. Quant. Grav. **17**, 2621 (2000); Int. J. Mod. Phys. D **10**, 477 (2001); M. Giovannini, Phys. Rev. D **82**, 083523 (2010); Class. Quant. Grav. **31**, 225002 (2014).
- [8] A. Abramovici *et al.*, Science **256**, 325 (1992); B. P. Abbott *et al.* [LIGO/Virgo Collaboration], Phys. Rev. Lett. **116**, no. 6, 061102 (2016); B. P. Abbott *et al.* [LIGO/Virgo Collaboration], arXiv:1602.03847 [gr-qc].
- [9] [Fermi-LAT Collaboration], arXiv:1602.04488 [astro-ph.HE]; P. A. Evans *et al.* [Swift Collaboration], arXiv:1602.03868 [astro-ph.HE]; J. Kanner, J. Camp, J. Racusin, N. Gehrels and D. White, Astrophys. J. **759**, 22 (2012).
- [10] M. Giovannini, Phys. Rev. D **58**, 083504 (1998); Phys. Rev. D **60**, 123511 (1999); Phys. Rev. D **59**, 121301 (1999).
- [11] S. Weinberg, Phys. Rev. D **69**, 023503 (2004); D. A. Dicus and W. W. Repko, Phys. Rev. D **72**, 088302 (2005); L. A. Boyle and P. J. Steinhardt, Phys. Rev. D **77**, 063504 (2008); Y. Watanabe and E. Komatsu, Phys. Rev. D **73**, 123515 (2006).
- [12] V. M. Kaspi, J. H. Taylor, and M. F. Ryba, Astrophys. J. **428**, 713 (1994); F. A. Jenet *et al.*, Astrophys. J. **653**, 1571 (2006); P. B. Demorest *et al.*, Astrophys. J. **762**, 94 (2013); R. M. Shannon *et al.*, Science **349**, no. 6255, 1522 (2015); W. Zhao, Phys. Rev. D **83**, 104021 (2011); W. Zhao, Y. Zhang, X.-P. You, Z.-H. Zhu, Phys. Rev. D **87**, 124012 (2013).
- [13] V. F. Schwartzmann, JETP Lett. **9**, 184 (1969); M. Giovannini, H. Kurki-Suonio and E. Sihvola, Phys. Rev. D **66**, 043504 (2002); R. H. Cyburt, B. D. Fields, K. A. Olive, and E. Skillman, Astropart. Phys. **23**, 313 (2005).
- [14] A. Arvanitaki and A. A. Geraci, Phys. Rev. Lett. **110**, no. 7, 071105 (2013); S. S. Seahra, C. Clarkson and R. Maartens, Phys. Rev. Lett. **94**, 121302 (2005); M. Servin and G. Brodin, Phys. Rev. D **68**, 044017 (2003); M. Servin, G. Brodin, M. Bradley and M. Marklund, Phys. Rev. E **62**, 8493 (2000).
- [15] A. M. Cruise, Class. Quantum Grav. **17**, 2525 (2000); P. Bernard, G. Gemme, R. Parodi and E. Picasso, Rev. Sci. Instrum. **72**, 2428 (2001); F. Y. Li, M. X. Tang and D. P. Shi, Phys. Rev. D **67**, 104008 (2003); A. M. Cruise and R. M. Ingley, Class. Quantum Grav. **23**, 6185 (2006); A. Nishizawa *et al.*, Phys. Rev. D **77**, 022002 (2008).